Corrosion characteristics of Al-Cu/B_4C (T6) MMCs and their microstructure evaluation

B. Dikici[1]*, F. Bedir[2], M. Gavgali[3], T. Kiyak[4]

[1] Yuzuncu Yil University, Ercis Technical Vocational School of Higher Education, 65400 Ercis-Van, Turkey
[2] Suleyman Demirel University, Department of Mechanical Engineering, 32260 Isparta, Turkey
[3] Ataturk University, Department of Mechanical Engineering, 25240 Erzurum, Turkey
[4] Gazi University, Art & Sciences Faculty, Department of Chemistry, 06500 Ankara, Turkey

Received 6 November 2008, received in revised form 8 July 2009, accepted 9 July 2009

Abstract

In this study, the pitting susceptibilities of Al-Cu alloy based metal matrix composites (MMCs) reinforced with boron carbide (B_4C) particles have been investigated using cyclic polarization (CP) technique in aerated and deaerated 3.5 wt.% NaCl solution. The effects of reinforcement particle volume fraction and artificially aged (T6) process on corrosion behaviour of the composites have been also examined. It has been found that the 30 % B_4C MMC is more susceptible to pitting attack compared with 10 % B_4C MMC.

Key words: MMC, particulate reinforced composites, corrosion, ageing, aluminium

1. Introduction

Aluminium alloys are used widely in aerospace and, more recently, in automotive industry as well as in defence industry. Ceramic particulate reinforced metal matrix composites (MMCs) have been the most popular ones for applications in these industrial branches. It is well known that boron carbide (B_4C) has some excellent physical and chemical properties, such as ultrahigh hardness, low density, excellent thermal stability, neutron absorption. So MMCs reinforcing B_4C particulates provide higher strength and stiffness, better thermal and creep properties and dimensional stability. However, B_4C is a very hard phase and extreme susceptible to brittle fracture [1–9].

Nowadays, ageing treatment has been widely used to increase the strength of Al-Cu alloys. Several corrosion studies [10–13] indicated that ageing treatment might affect greatly the corrosion behaviour of MMCs. Lucas and Clarke [1] summarized that the composition, volume fraction, location, and potential of the precipitates (or micro constituents) have a direct effect on the amount, form and distribution of the corrosion attack of the MMC. For example, the formation of $CuAl_2$ precipitates during ageing in Al-Cu based alloys alters the pitting characteristics of the matrix alloy, and therefore their composites. Hollingsworth et al. [14] report that solution potential of $CuAl_2$ is −730 mV (vs. SCE) and the value is more noble than solution potential of aluminium (−840 mV vs. SCE) in high concentration sodium chloride (NaCl) solution. In other words, $CuAl_2$ phases act as the cathode in Cu-containing Al alloys and this stems from potential differentiations in Al alloys or its composites [1]. Consequently, Al-Cu based alloys or its composites are more susceptible to pitting corrosion. On the other hand, electrochemical behaviour of boron is the same as $CuAl_2$ precipitates in Al alloys. Pohlman [15] investigated corrosion susceptibilities of boron fibre (B_f) reinforced AA2024 composites for different ageing times in 3.5 % NaCl solutions [1]. He found that the fibre/matrix interface was preferentially attacked in the composites. In addition, deposition of oxide films of copper on the matrix alloy surface enhances corrosion activities of these materials because Cu forms p-type oxide on the surface, of which its electrical conductivity increases with the oxygen pressure, whereas Al forms n-type oxide on the surface, of which its electrical conductivity decreases with the oxygen pressure [16, 17]. Thus, the oxide layer is more

---

*Corresponding author: tel.: +90 388 2164 (5042); fax: +90 432 388 2165; e-mail address: burakdikici@yyu.edu.tr

Table 1. Open circuit (E_{ocp}), corrosion (E_{corr}), pitting potentials (E_{pit}), and corrosion current density (i_{corr}) values of unaged and aged (T6) composites in aerated 3.5 % NaCl solution

Material	E_{ocp} (mV)	E_{corr} (mV)	E_{pit} (mV)	i_{corr} (μA cm^{-2})
10 % B_4C MMC	–672	–624	–605	4.2
30 % B_4C MMC	–678	–635	–626	6.0
10 % B_4C MMC-T6	–625	–586	–577	3.8
30 % B_4C MMC-T6	–635	–596	–582	5.7

complex when compared with unageing conditions. Notwithstanding above studies, the published research works on the corrosion of MMCs reinforced with B_4C particles are rather limited.

Our previous studies [3, 4, 17, 18] were focused on the role of SiC and TiC particle reinforcements on the corrosion behaviour of the aluminium. Therefore, the aim of the experimental study is to calculate the pitting and reverse potential (E_{pit} and E_{rp}) and to study the effect of artificially aged (T6) on the corrosion characteristics of Al-Cu/B_4C MMCs in 3.5 % NaCl solutions.

2. Experimental procedure

The composites reinforced with B_4C particles at weight percents of 10 and 30 % were produced by using conventional hot press method and then artificially aged (T6). The matrix alloy used in this work is aluminium-based alloy containing 5 wt.% Cu. The details of the production method and ageing process were given in the previous study [19].

The corrosion susceptibility of each material was analysed by measurements of the cyclic and potentiodynamic polarizations. The pitting kinetics of the composites was obtained from the polarization graphics. In this study, ASTM standards (G 1 and G 5) are used for checking the experimental technique and instrumentation and the prepared corrosion test specimens [20, 21]. The all electrochemical measurements were carried out using a PGS95 potentiostat/galvanostat (BANK Inc., Germany) in aerated and deaerated 3.5 wt.% NaCl solution at room temperature. An Ag/AgCl electrode and platinum (Pt) electrode were used as reference and auxiliary electrodes, respectively. The specimens were ground successively from 400 to 1200 grit and immersed into the solution until a steady open circuit potential (OCP) was obtained. After equilibration, PDS and CP tests were started at a rate of 10 mV min^{-1}. The solution was deaerated to remove oxygen with N_2 gas. The deaerated process started 60 minutes prior to measurement and continued until the end of the experiment. After polarization, specimens were ultrasonically cleaned with distilled water for metallographic observations. The corroded surfaces were examined using a scanning electron microscope (SEM). In addition, phase identification of the composites is performed by using an X-ray diffraction (XRD, Rigaku) with Cu Kα radiation.

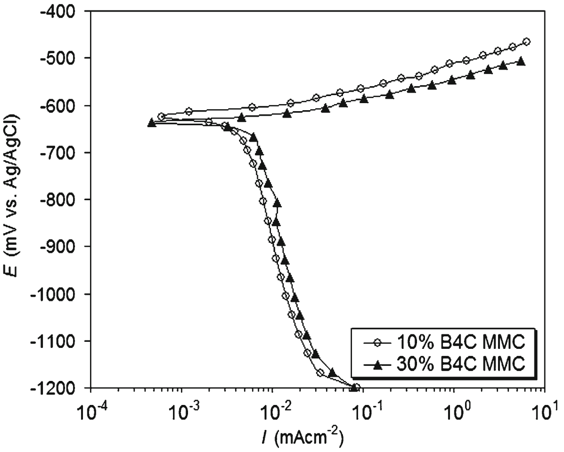

Fig. 1. PDS curves of unaged composites in aerated solution.

3. Results

Potentiodynamic scanning (PDS) curves of both unaged and aged (T6) composites in aerated solution are given in Figs. 1 and 2, which show the effect of B_4C ratios on the corrosion resistance.

In addition, the E_{corr}, E_{pit} and i_{corr} values calculated from the polarization curves, in which the experiment was carried out in 3.5 % NaCl/laboratory atmosphere, are presented in Table 1.

Table 1 indicates that the corrosion resistances (E_{corr}, i_{corr}) of the composites decrease with the increase of B_4C volume fraction in both unaged and aged conditions. In addition, it can be clearly seen that the corrosion potential approaches closely to the pitting potential because of subtle polarization effect in aerated conditions. Therefore, in the second stage of the study, all electrochemical tests were repeated under nitrogen (N_2) atmosphere. Cyclic polarization (CP) curves of the unaged and aged composites after

Table 2. Potential and current density values of the unaged and aged composites in deaerated 3.5 % NaCl solution

Material	E_{ocp} (mV)	E_{corr} (mV)	E_{pit} (mV)	E_{rp} (mV)	i_{corr} (μA cm^{-2})
10 % B_4C MMC	–709	–1008	–528	–717	1.2
30 % B_4C MMC	–690	–968	–604	–748	3.0
10 % B_4C MMC-T6	–672	–979	–541	–748	1.0
30 % B_4C MMC-T6	–677	–828	–559	–718	2.1

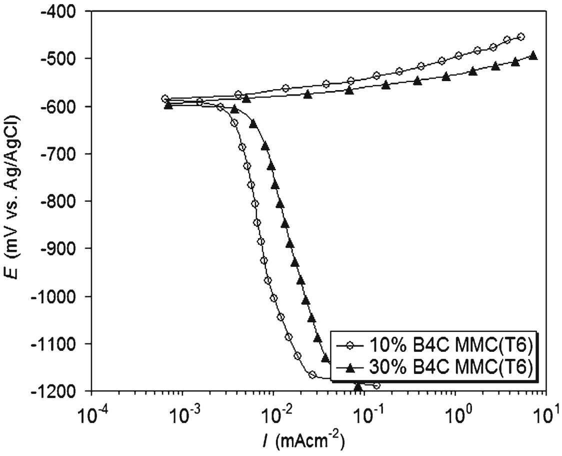

Fig. 2. PDS curves of aged composites in aerated solution.

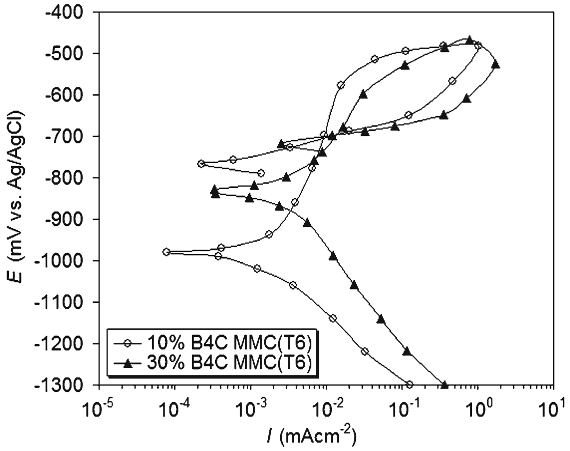

Fig. 4. CP curves of aged composites in deaerated solution.

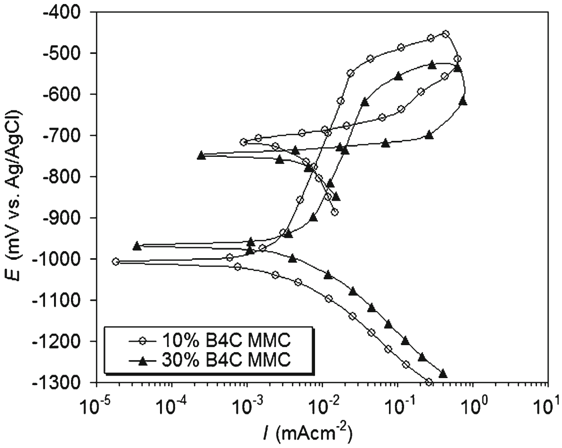

Fig. 3. CP curves of unaged composites in deaerated solution.

deaerated process are compared in Figs. 3 and 4. In these curves, the pitting potentials (E_{pit}) could be easily determined by a marked rise in the anodic current density for the each particle volume fraction.

The E_{corr}, E_{pit}, E_{rp} (reverse potential) and i_{corr} values calculated from the curves are given in Table 2.

CP curve hysteresis can provide information on pitting corrosion rates and how rapidly a passive film repairs itself. All polarization curves in Figs. 3 and 4 have a positive hysteresis because the reverse scan current densities are greater than those of forward scan. Also, the hysteresis loops of the polarization curves of the unaged composites are of smaller size in comparison with the T6 tempered composites. From Table 2, it can be seen that the i_{corr} values of the materials that increased with increasing B4C particle fraction did not increase with ageing. The behaviour is the same as for aerated solutions (Table 1). On the other side, the maximum value of i_{corr} reaches 3.0 μA cm^{-2} in unaged 30 % B_4C MMC, but the value is smaller than i_{corr} values in Table 1.

Corroded surfaces of the composites are given in Fig. 5, where developing pit cell sizes were determined in the range of 175–250 μm and 75–200 μm for 10 vol.% and 30 vol.% B_4C_p composites, respectively.

Metallographic observations on the composite surfaces indicate preferentially corrosion formed around B_4C particles (Fig. 6a). In addition, pits on the matrix constituent of the composites were generally rounded edge, crystallographic, widespread and irregular shape as seen from Fig. 6b. In addition, XRD results also indicate that Al_4C_3 phase is not formed during the fabrication and/or ageing of the composites (Fig. 7).

4. Discussion

In aerated conditions, the corrosion rate (i_{corr}) of

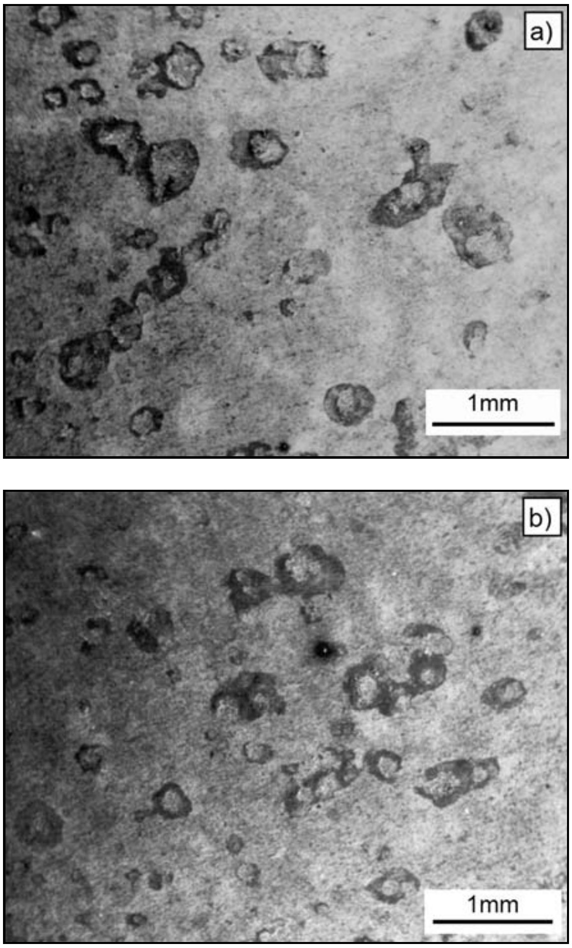

Fig. 5. SEM morphology of a) 10 vol.% B_4C and b) 30 vol.% B_4C composites.

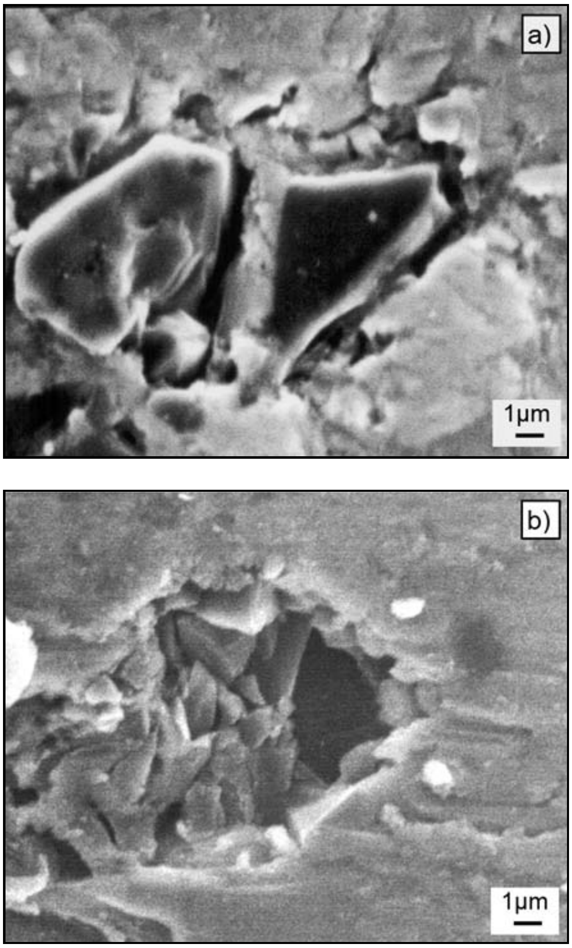

Fig. 6. a) Preferentially corrosion formed around B_4C particles in the 10 vol.% B_4C composite and b) established pit on the 30 vol.% B_4C composite in the T6 conditions.

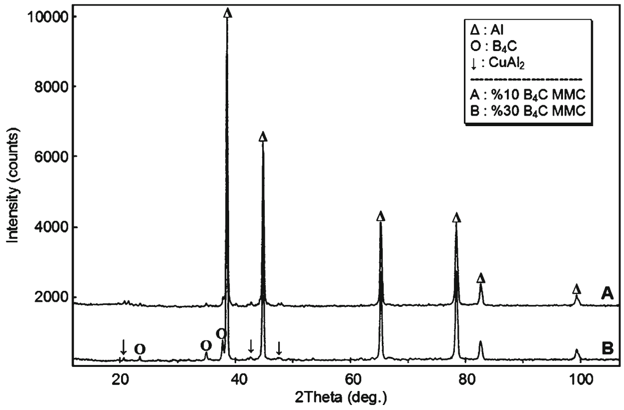

Fig. 7. XRD patterns of the aged composites.

30 vol.% B_4C composite for any potential value in the anodic polarization zone (Figs. 1 and 2) is higher than that of 10 vol.% B_4C composite. In other words, the oxide film resistance of the surface decreases with increasing B_4C volume fraction. These results are in accordance with composite theory because it is well known that the presence of reinforcement in the matrix alloy may cause cracks and discontinuity on the surface oxide layer that increase with increasing reinforcement volume fraction [11, 22]. In Fig. 6a, the corrosion occurred principally at the matrix alloy/B_4C interfaces because the surface oxide film in these areas was defective.

The X-ray mappings taken in the SEM indicate that Cu content is relatively high at the matrix/reinforcement interfaces (Fig. 8). The copper is an essential component in producing the high strength ageing alloys [14, 23]. However, it seriously diminishes the corrosion resistance of Al alloys. Hollingsworth et al. [14] report that solution potential of $CuAl_2$ is −730 mV and the value is nobler than solution potential of aluminium (–840 mV). $CuAl_2$ precipitations formed on the matrix/reinforcement interfaces with ageing (T6) may have enhanced corrosion susceptibility of the composites (Fig. 7). In other words, the noble components ($CuAl_2$) gathered due to segregation increase the ratio of local cathode area at the

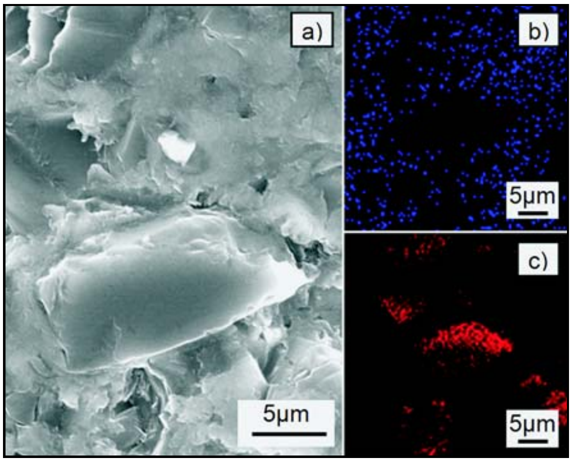

Fig. 8. a) SEM image and the X-ray maps of b) Cu and c) B of 30 vol.% B_4C composite.

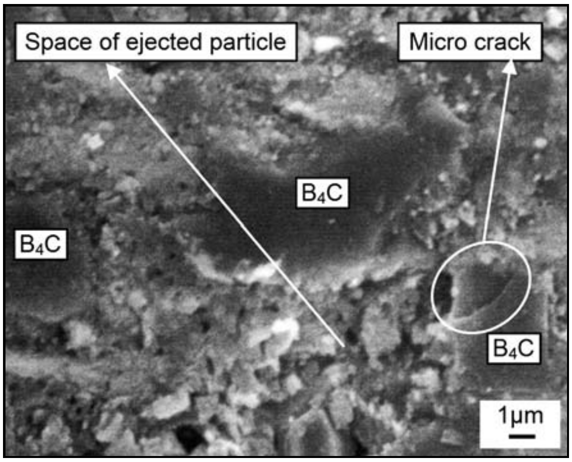

Fig. 9. Micro-cracks and disespoused place of boron carbide due to intensive matrix corrosion in T6 heat-treated 30 vol.% B_4C composite.

B_4C/matrix interfaces when the potential exceeds the E_{pit} value, corrosion may start in these points [1, 14] (Fig. 5).

It can be clearly seen from Table 1 that the corrosion potential approaches closely the pitting potential. Therefore, it is very difficult to completely determine the effect of polarization. In this case, deaerated process has been carried out in the corrosion cell. The process provides a convenient, reliable method for the determination of pitting and protection potentials [24]. As seen from Figs. 3, 4 and Table 2, both the i_{corr} and E_{pit} values of the composites increase negatively with increasing the B_4C volume fraction in both unaged and aged conditions. In the case of considering these results together, it can be concluded that 10 vol.% B_4C composite exhibits higher corrosion resistance than that of 30 vol.% B_4C composite (Figs. 5 and 6).

According to Trowsdale et al. [10], a significant contribution to increasing the pitting susceptibility of the composites is the presence of voids and crevices because of altering the normal pitting behaviour of the MMCs. It is well known that during the fabrication of particle reinforced MMCs, reinforcements may crack or break into pieces and in the case of the potential of composite exceeds E_{pit}, pitting may form and grow at these cracks [3, 25]. In addition, areas, which have different potentials, may increase, and when the potential exceeds E_{corr} value, as a result these areas may act as corrosion nucleation sites [1, 26]. Similar results were also obtained in the previous studies [3, 4] and were in agreement with the depictions observed by Turnbull [13]. In the present study, the porosity values in sintered condition under pressure for all types of material are below 2 % [27]. However, the presence of micro-cracked particles can form preferentially induced corrosion mechanism. In this case, the corrosion will continue around these particles and also provide the development of main pits. At the advanced stages of the corrosion, the pit extends in-depth and ejects the reinforcements from the structure as seen in Fig. 9.

Some research groups reported that the pitting potential itself was insufficient to access the likelihood of pitting [1, 28, 29]. In addition, Nisancioglu and Holton [30] argued that E_{pit} could not be used as a criterion for determining the pitting susceptibility of aluminium alloys. Therefore, determination of E_{rp} (or protection potential, E_{prot}) in chloride medium provides a rapid means of evaluating the material for its resistance to localized corrosion. The ability to repassivation during reverse scan suggests that the composites develop passive film with ability to repair itself and during the forward scan this ability also helps to achieve a more noble pitting potential. When the potential exceeds the E_{rp} value, the equilibrium condition is lost during polarization, which causes change in current density, hence rupture in protective films. While the parameter (E_{pit}-E_{corr}) is a measure of the extent of the passive region on the polarization curve and provides an indication of the susceptibility to pitting in deaerated solution, the parameter (E_{pit}-E_{rp}) is used to assess the repassivation behaviour of propagation pits, hence active sites can easily be eliminated locally [10]. A decrease in value of the (E_{pit}-E_{rp}) from 207 mV in 10 vol.% B_4C composite to 159 mV in 30 vol.% B_4C composite is calculated in the aged condition (Table 2). The possible reasons for this change in electrochemical behaviour can be B_4C volume fraction and/or T6 heat treatments as mentioned above. On the other hand, the hysteresis loop of polarization curves of the unaged composites (Fig. 3) is smaller when compared to the aged composites (Fig. 4). This accounts for the easier repassivation tendency due to the absence of B_4C particles, which can act as a cathode in irritating the growth of the pits. The

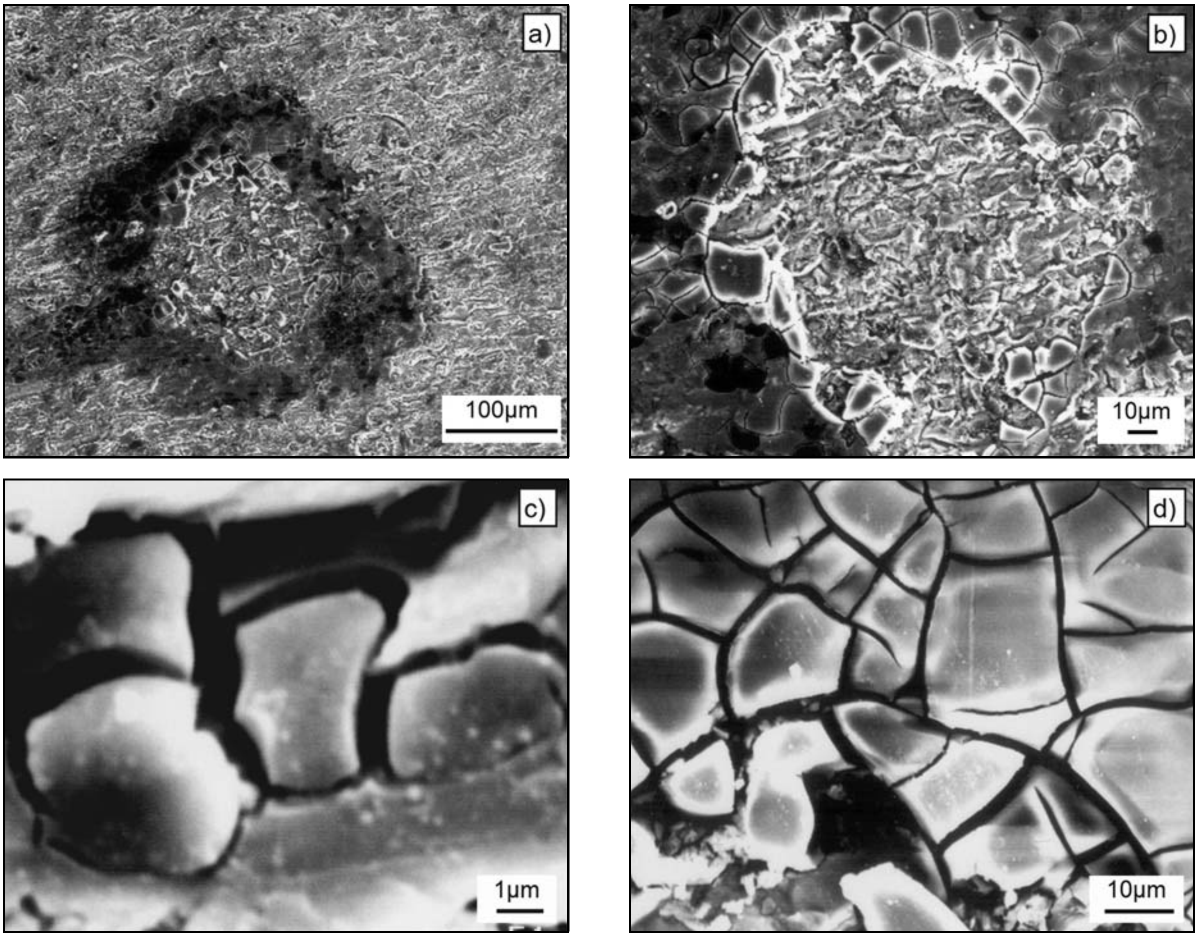

Fig. 10. Micro-submicro local batteries in a) the 10 vol.% and b) 30 vol.% B_4C composites and typical oxide micrographs of c) the 10 vol.% and d) 30 vol.% B_4C composites.

pit sizes also decreased with increasing B_4C content, probably due to B_4C particles, which are acting as physical barriers to the corrosion process (Fig. 5). B_4C particle reflects property of noble characteristic in the aluminium matrix and does not undergo corrosion (Fig. 6a). Meanwhile, the structure tends to induce many micro-submicro local batteries, and causes the matrix grains potentially differentiate (Fig. 10a,b), thus increases the pitting potential. This behaviour may cause to form the small anode-big cathode corrosion type and the corrosion increase significantly. This process progresses quickly and continues until the matrix degradation. The following reactions take part in this process:

$$\mathrm{Al} \rightarrow \mathrm{Al}^{3+} + 3\mathrm{e}^-, \tag{1}$$

$$\mathrm{Al}^{3+} + 3\mathrm{H_2O} \rightarrow \mathrm{Al(OH)_3} + 3\mathrm{H}^+. \tag{2}$$

After oxidizing of Al^{3+} ions according to reaction (1) and (2), they will react with Cl^- ions and transform to aluminium chloride according to the reactions (3), (4) and (5). This may cause an increase in the solubility of the oxide film (Fig. 10c,d) [19, 20, 31]:

$$\mathrm{Al(OH)_3} + \mathrm{Cl}^- \rightarrow \mathrm{AlCl(OH)_2} + \mathrm{OH}^-, \tag{3}$$

$$\mathrm{AlCl(OH)_2} + \mathrm{Cl}^- \rightarrow \mathrm{AlCl_2OH} + \mathrm{OH}^-, \tag{4}$$

$$\mathrm{AlCl_2OH} + \mathrm{Cl}^- \rightarrow \mathrm{Al}^{3+} + 3\mathrm{Cl}^- + \mathrm{OH}^-. \tag{5}$$

5. Conclusion

The experimental study showed that the 30 % B_4C MMC was more susceptible to pitting attack compared with 10 % B_4C MMC. In addition, the following conclusions can be drawn from the above study:

1. The polarization results show that the B_4C and its volume fraction have a great effect on the electrochemical behaviour of the composites in 3.5 % NaCl solution.

2. (E_{pit}-E_{rp}) parameter must be used to determine the tendency of the active metal dissolution in the media.

3. From the cyclic potentiodynamic polarization curves and SEM images, when the potential has reached the E_{rp}, the active site on the aluminium surface was blocked and the surface oxide film repaired itself by corrosion products.

4. The SEM images show preferentially corrosion formed around B_4C particles in the composites probably because of the $CuAl_2$ precipitation phases.

Acknowledgements

This work was supported by TUBITAK (The Scientific & Technological Research Council of Turkey, MAG 106M156) and Ataturk University (BAP No: 2005/14).

References

[1] LUCAS, K. A.—CLARKE, H.: Corrosion of Aluminium-Based Metal Matrix Composites. Chichester, Wiley 1993.

[2] HUDA, M. D.—HASHMI, M. S. J.—EL-BARADIE, M. A.: Key Engineering Materials, *104–107*, 1995, p. 37.

[3] DIKICI, B.—GAVGALI, M.—TEKMEN, C.: Journal of Composite Materials, *40*, 2006, p. 1259.

[4] GAVGALI, M.—DIKICI, B.—TEKMEN, C.: Corrosion Reviews, *24*, 2006, p. 27.

[5] LEE, K. B.—SIM, H. S.—CHO, S. Y.—KWON, H.: Materials Science and Engineering, *A302*, 2001, p. 227.

[6] LLOYD, D. J.—JIN, I.: Comprehensive Composite Materials, *3*, 2000, p. 555.

[7] JIANG, Q. C.—WANG, H. Y.—MA, B. X.—WANG, Y.—ZHAO, F.: Journal of Alloys and Compounds, *386*, 2005, p. 177.

[8] ARSLAN, G.—KARA, F.—TURAN, S.: Journal of the European Ceramic Society, *23*, 2003, p. 1243.

[9] LASAGNI, F.—DEGISCHER, H. P.—PAPAKYRIACOU, M.: Kovove Mater., *44*, 2006, p. 65.

[10] TROWSDALE, A. J.—NOBLE, B.—HARIS, S. J.—GIBBINS, I. S. R.—THOMPSON, G. E.—WOOD, G. C.: Corrosion Science, *38*, 1996, p. 177.

[11] MCINTYRE, J. F.—CONRAD, R. K.—GOLLEDGE, S. L.: Corrosion, *46*, 1990, p. 902.

[12] DE SALAZAR, J. M. G.—URENA, A.—MANZANEDO, S.—BARRENA, M. I.: Corrosion Science, *41*, 1999, p. 529.

[13] TURNBULL, A.: British Corrosion Journal, *27*, 1992, p. 27.

[14] HOLLINGSWORTH, H.—HUNSICKER, Y. H.: ASM Handbook 13. Ohio, ASM 1987.

[15] POHLMAN, S. L.: Corrosion, *34*, 1978, p. 156.

[16] SHREIR, L. L.: Corrosion. Singapore, Tien Wah Press 1979.

[17] GAVGALI, M.—DIKICI, B.—BEDIR, F.: Indian Journal of Engineering and Materials Science, *14*, 2007, p. 303.

[18] DIKICI, B.—TEKMEN, C.—YIGIT, O.—GAVGALI, M.—COCEN, U.: Corrosion Science, *51*, 2009, p. 469.

[19] BEDIR, F.—OGEL, B.—GURBUZ, R.: Metall, *59*, 2005, p. 459.

[20] ASTM G1: Annual Book of ASTM Standards. Pennsylvania, ASTM 2001.

[21] ASTM G5: Annual Book of ASTM Standards. Pennsylvania, ASTM 2001.

[22] BHAT, M. S. N.—SURAPPA, M. K.: Journal of Materials Science, *26*, 1991, p. 4991.

[23] TALBOT, D.—TALBOT, J.: Corrosion Science and Technology. Florida, Boca Raton, CRC Press 1998.

[24] GALVELE, J. R.: Corrosion Science, *47*, 2005, p. 3053.

[25] DIKICI, B.: Corrosion Behaviours of Al-Si-Mg Based SiC Particle Reinforced Metal Matrix Composites. [Master Thesis]. Erzurum, Turkey, Ataturk University 2004.

[26] AHMED, Z.—ABDUL ALEEM, B. J.: Materials Design, *23*, 2002, p. 173.

[27] GAVGALI, M.—DIKICI, B.—BEDIR, F.: In: X. International Corrosion Symposium. Ed.: Erbil, M. Turkey, Adana, Çukurova University 2006, p. 207.

[28] NILSEN, N.—BARDAL, E.: Corrosion Science, *17*, 1977, p. 635.

[29] OTANI, T.—MCENANEY, B.—SCOTT, V. D.: In: Proc. Int. Symp. on Cast Reinforced Metal Composites. Eds.: Fishman, S. G., Dhingra, A. K. Materials Park, OH, ASM International 1988, p. 383.

[30] NISANCIOGLU, K.—HOLTON, H.: Corrosion Science, *18*, 1977, p. 635.

[31] KIYAK, T.: The Investigation of Temperature Dependence of Aluminium (Cathodic) Corrosion at pH 4-6. [PhD Dissertation]. Ankara, Turkey, Gazi University 1995.